Received: 31 May 2024 | Revised: 2 November 2024 | Accepted: 4 November 2024

DOI: 10.1002/pamm.202400201

PAMM Proceedings in Applied Mathematics and Mechanics

RESEARCH ARTICLE

# A divergence-conforming method for flow and double-diffusive transport

**Raimund Bürger**[1] | **Arbaz Khan**[2] | **Paul E. Méndez**[3] | **Ricardo Ruiz-Baier**[4,5,6]

[1]CI²MA and Departamento de Ingeniería Matemática, Universidad de Concepción, Concepción, Chile

[2]Department of Mathematics, Indian Institute of Technology Roorkee, Roorkee, India

[3]Research Centre on Mathematical Modelling (MODEMAT), Escuela Politécnica Nacional, Quito, Ecuador

[4]School of Mathematics, Monash University, Melbourne, Australia

[5]World-Class Research Center "Digital biodesign and personalized healthcare", Sechenov First Moscow State Medical University, Moscow, Russia

[6]Universidad Adventista de Chile, Chillán, Chile

**Correspondence**
Raimund Bürger, CI2MA and Departamento de Ingeniería Matemática, Universidad de Concepción, Casilla 160-C, Concepción, Chile.
Email: rburger@ing-mat.udec.cl

**Funding information**
ANID: CRHIAM, Grant/Award Numbers: ANID/FONDAP/15130015, ANID/FONDAP/1523A0001, ANID/ACT210030, Fondecyt 1210610; Sponsored Research & Industrial Consultancy, Grant/Award Number: MTD/FIG/100878; SERB, Grant/Award Numbers: MTR/2020/000303, CRG/2021/002569; Monash Mathematics Research Fund, Grant/Award Number: S05802-3951284; Higher Education of the Russian Federation, Grant/Award Number: 075-15-2022-304; Australian Research Council, Grant/Award Numbers: FT220100496, DP22010316

**Abstract**
The results of a recent extension of the analysis of an $\mathbf{H}(\mathrm{div})$-conforming method for a model of double-diffusive flow in porous media introduced in [Bürger, Méndez, Ruiz-Baier, SINUM (2019), 57:1318–1343] to the time-dependent case are summarized. These include the efficiency and reliability of residual-based a posteriori error estimators for the steady, semi-discrete, and fully discrete problems. The method consists of Brezzi–Douglas–Marini approximations for velocity and compatible piecewise discontinuous pressures, whereas Lagrangian elements are used for concentration and salinity. Novel numerical tests confirm the accuracy of the method and illustrate its application to a salinity-driven problem of sedimentation.

## 1 | INTRODUCTION AND PROBLEM FORMULATION

### 1.1 | Scope

We are interested in numerical schemes for coupled equations that model the sedimentation of small particles under the effect of salinity of the fluid. The governing model (e.g., [14, 26]) of coupled incompressible flow and double-diffusion transport is

$$\partial_t \boldsymbol{u} + \boldsymbol{u} \cdot \boldsymbol{\nabla} \boldsymbol{u} = \mathbf{div}\big(\nu(c)\boldsymbol{\nabla}\boldsymbol{u}\big) - (1/\rho_{\mathrm{m}})\nabla p + (\rho/\rho_{\mathrm{m}})\boldsymbol{g}, \quad \operatorname{div} \boldsymbol{u} = 0, \tag{1.1a}$$

$$\partial_t s + \boldsymbol{u} \cdot \nabla s = (1/\mathrm{Sc})\Delta s, \quad \partial_t c + (\boldsymbol{u} - v_{\mathrm{p}}\boldsymbol{e}_z) \cdot \nabla c = (1/(\tau\mathrm{Sc}))\Delta c, \tag{1.1b}$$

  

posed on a spatial domain $\Omega \subset \mathbb{R}^d$, $d = 2$ or $d = 3$, where $t \in (0, t_{\text{end}}]$ is time, $\boldsymbol{u}$ is the fluid velocity, $\nu$ is the concentration-dependent viscosity, $\rho_{\text{m}}$ is the mean density of the fluid, $p$ is the fluid pressure, $\rho$ is density, $\boldsymbol{g}$ is the gravity acceleration, $s$ is the salinity concentration, and $c$ is the concentration of solid particles. The Schmidt number $\text{Sc} = \nu_{\text{ref}}/\kappa_{\text{s}}$ is assumed relatively small, for example, $\text{Sc} = \mathcal{O}(10)$. Finally, $\kappa_{\text{s}}$ is the diffusivity of salinity, $\nu_{\text{ref}}$ is a reference viscosity in the absence of solid particles, $\tau = \kappa_{\text{s}}/\kappa_{\text{c}}$, where $\kappa_{\text{c}}$ is the diffusivity of solid particles, and $\boldsymbol{e}_z$ is the upward-pointing unit vector. A linearized equation of state $\rho = \rho_{\text{m}}(\alpha s + \beta c)$ is assumed. The particles are assumed to settle at a constant dimensionless velocity $v_{\text{p}}$.

Recent finite element and related schemes for double-diffusive flows include refs. [6, 8, 13, 16, 17, 24, 28]. The solvability analysis for the continuous and discrete problems usually follows energy and fixed-point arguments; this is also the approach of ref. [12]. The discretization in space uses an interior penalty divergence-conforming method for the flow equations (here, Brezzi–Douglas–Marini (BDM) elements of degree $k \geq 1$ for $\boldsymbol{u}$ and discontinuous elements of degree $k-1$ for $p$, cf. [7, 22]), combined with Lagrangian elements for $s$ and $c$. This treatment extends that of ref. [13] to the transient case. The proposed method also features exactly divergence-free velocity approximations ensuring local conservativity and energy stability, and the error estimates of velocity are pressure-robust. The chosen time discretization is the backward differentiation formula of degree 2 (BDF2), which for $k = 2$ gives a method of order 2 in space and time. Existence of discrete solutions follows by a fixed-point argument (cf. [13]), and the error analysis adapted from refs. [2, 8]. We herein summarize the analysis of ref. [12] and present two new numerical examples, namely one accuracy test and a simulation of salinity-driven sedimentation.

For salinity-driven sedimentation many flow features (e.g., plumes) are clustered near high gradients of concentration [14, 24]. This motivates adaptive mesh refinement guided by a posteriori error indicators [17, 25]. Most literature on residual-based a posteriori error estimators for flow-transport couplings is focused on the stationary case (e.g. [1, 3–5, 18, 27]). None of the (few) analyzes for the time-dependent case (e.g. [9, 10, 23]) applies to divergence-conforming approximations to (1.1).

The a posteriori error analysis we advance here is of residual type. The approach hinges on a decomposition of the discrete solution into a conforming and a non-conforming contribution, along with a reconstruction technique. The error analysis is divided into three parts. In the first part, we present the error estimator for the steady coupled problem. In second part, we extend the a posteriori error estimation to the semi-discrete method, and finally we present the a posteriori error estimator for the unsteady coupled problem. For the sake of simplicity, we restrict the latter analysis to the backward Euler method.

## 1.2 | Preliminaries, additional assumptions, and weak formulation

Let $\Omega$ be an open and bounded domain in $\mathbb{R}^d$, $d = 2, 3$ with Lipschitz boundary $\Gamma = \partial\Omega$. We denote by $L^p(\Omega)$ and $W^{r,p}(\Omega)$ the usual Lebesgue and Sobolev spaces, write $H^r(\Omega) = W^{r,2}(\Omega)$, and denote the corresponding norm by $\|\cdot\|_{r,\Omega}$ ($\|\cdot\|_{0,\Omega}$ for $H^0(\Omega) = L^2(\Omega)$). The space $L^2_0(\Omega)$ denotes the restriction of $L^2(\Omega)$ to functions with zero mean value over $\Omega$. For $r \geq 0$, we write the $H^r$-seminorm as $|\cdot|_{r,\Omega}$ and denote by $(\cdot,\cdot)_\Omega$ the usual inner product in $L^2(\Omega)$. Spaces of vector-valued functions are denoted in bold face, that is, $\boldsymbol{H}^r(\Omega) = [H^r(\Omega)]^d$, and we use the vector-valued Hilbert spaces $\boldsymbol{H}(\text{div};\Omega) := \{\boldsymbol{w} \in \boldsymbol{L}^2(\Omega) : \text{div}\,\boldsymbol{w} \in L^2(\Omega)\}$, $\boldsymbol{H}_0(\text{div};\Omega) := \{\boldsymbol{w} \in \boldsymbol{H}(\text{div};\Omega) : \boldsymbol{w}\cdot\boldsymbol{n}_{\partial\Omega} = 0 \text{ on } \partial\Omega\}$ and $\boldsymbol{H}_0(\text{div}^0;\Omega) := \{\boldsymbol{w} \in \boldsymbol{H}_0(\text{div};\Omega) : \text{div}\,\boldsymbol{w} = 0 \text{ in } \Omega\}$, where $\boldsymbol{n}_{\partial\Omega}$ is the outward normal on $\partial\Omega$. We endow these spaces with the norm $\|\boldsymbol{w}\|^2_{\text{div},\Omega} := \|\boldsymbol{w}\|^2_{0,\Omega} + \|\text{div}\,\boldsymbol{w}\|^2_{0,\Omega}$. We denote by $L^s(0,t_{\text{end}};W^{m,p}(\Omega))$ the Banach space of all $L^s$-integrable functions from $[0,t_{\text{end}}]$ into $W^{m,p}(\Omega)$.

As in, for example [18], we assume that viscosity is a Lipschitz continuous and uniformly bounded function of $c$.

For simplicity of presentation we restrict the weak form to the homogeneous Dirichlet boundary conditions $\boldsymbol{u} = \boldsymbol{0}$, $s = 0$, and $c = 0$ on $\partial\Omega$. Furthermore, we define the spaces $\boldsymbol{V}^t := \{\boldsymbol{w} \in \boldsymbol{L}^2(0,t_{\text{end}};\boldsymbol{H}^1_0(\Omega)) : \partial_t\boldsymbol{w} \in L^2(0,t_{\text{end}}\boldsymbol{L}^2(\Omega))\}$, $Q^t := L^2(0,t_{\text{end}};L^2_0(\Omega))$, and $M^t := \{s \in L^2(0,t_{\text{end}};H^1_0(\Omega)) : \partial_t s \in L^2(0,t_{\text{end}};L^2(\Omega))\}$. For ease of presentation we furthermore assume that velocity, pressure, concentration and salinity solutions belong to $\boldsymbol{V}^t$, $Q^t$, $M^t$, and $M^t$, respectively. Testing each equation in (1.1) against suitable functions and integrating by parts gives the following weak formulation: Find $(\boldsymbol{u},p,s,c) \in \boldsymbol{V}^t \times Q^t \times M^t \times M^t$ such that $\boldsymbol{u}(\cdot,0) = \boldsymbol{u}_0 \in \boldsymbol{H}_0(\text{div}^0;\Omega)$, $s(\cdot,0) = 0$, $c(\cdot,0) = 0$ in $\Omega$ and

$$
\begin{aligned}
&(\partial_t\boldsymbol{u},\boldsymbol{v})_\Omega + a_1(c;\boldsymbol{u},\boldsymbol{v}) + c_1(\boldsymbol{u};\boldsymbol{u},\boldsymbol{v}) + b(\boldsymbol{v},p) = F(s,c,\boldsymbol{v}) \quad \forall\boldsymbol{v} \in \boldsymbol{H}^1_0(\Omega), \quad b(\boldsymbol{u},q) = 0 \quad \forall q \in L^2_0(\Omega), \\
&(\partial_t s,\varphi)_\Omega + a_2(s,\varphi) + c_2(\boldsymbol{u};s,\varphi) = 0, \quad (\partial_t c,\psi)_\Omega + \frac{1}{\tau}a_2(c,\psi) + c_2(\boldsymbol{u} - v_{\text{p}}\boldsymbol{e}_z;c,\psi) = 0 \quad \forall\varphi,\psi \in H^1_0(\Omega)
\end{aligned}
\tag{1.2}
$$

for a.e. $t \in [0, t_{\text{end}}]$, where for all $\boldsymbol{u}, \boldsymbol{v}, \boldsymbol{w} \in \boldsymbol{H}_0^1(\Omega)$, $q \in L_0^2(\Omega)$, and $\varphi, \psi \in H_0^1(\Omega)$, the variational forms are defined as

$$\begin{aligned} a_1(c; \boldsymbol{u}, \boldsymbol{v}) &:= \big(\nu(c)\boldsymbol{\nabla}\boldsymbol{u}, \boldsymbol{\nabla}\boldsymbol{v}\big)_\Omega, \quad c_1(\boldsymbol{w}; \boldsymbol{u}, \boldsymbol{v}) := \big((\boldsymbol{w}\cdot\boldsymbol{\nabla})\boldsymbol{u}, \boldsymbol{v}\big)_\Omega, \quad F(s, c, \boldsymbol{v}) := \big((\alpha s + \beta c)\boldsymbol{g}, \boldsymbol{v}\big)_\Omega, \\ b(\boldsymbol{v}, q) &:= -(1/\rho_{\mathrm{m}})(q, \operatorname{div}\boldsymbol{v})_\Omega, \quad a_2(\varphi, \psi) := (1/\mathrm{Sc})(\nabla\varphi, \nabla\psi)_\Omega, \quad c_2(\boldsymbol{v}; \varphi, \psi) := \big((\boldsymbol{v}\cdot\nabla)\varphi, \psi\big)_\Omega. \end{aligned} \tag{1.3}$$

## 1.3 | Stability of the continuous problem

The variational forms (1.3) are continuous for all $\boldsymbol{u}, \boldsymbol{v}, \in \boldsymbol{H}_0^1(\Omega)$, $q \in L_0^2(\Omega)$, and $\varphi, \psi \in H_0^1(\Omega)$, that is, there exist constants $C_a$ and $\hat{C}_a$ such that $|a_1(\cdot, \boldsymbol{u}, \boldsymbol{v})| \le C_a \|\boldsymbol{u}\|_{1,\Omega}\|\boldsymbol{v}\|_{1,\Omega}$, $|a_2(\varphi, \psi)| \le \hat{C}_a\|\varphi\|_{1,\Omega}\|\psi\|_{1,\Omega}$ and similar estimates for $b$, $c_1$, and $c_2$. The Poincaré–Friedrichs inequality $\|\varphi\|_{0,\Omega} \le C_p|\varphi|_{1,\Omega}$ for all $\varphi \in H_0^1(\Omega)$ implies the coercivity of $a_2$ and also, for a fixed concentration, that of $a_1$. By the characterization of the kernel of $b(\cdot,\cdot)$, we can write $\boldsymbol{X} := \{\boldsymbol{v} \in \boldsymbol{H}_0^1(\Omega) : b(\boldsymbol{v}, q) = 0 \quad \forall q \in L_0^2(\Omega)\} = \{\boldsymbol{v} \in \boldsymbol{H}_0^1(\Omega) : \operatorname{div}\boldsymbol{v} = 0 \text{ in } \Omega\}$, and an integration by parts reveals that $c_1(\boldsymbol{w}; \boldsymbol{v}, \boldsymbol{v}) = 0$ and $c_2(\boldsymbol{w}; \varphi, \varphi) = 0$ for all $\boldsymbol{w} \in \boldsymbol{X}, \boldsymbol{v} \in \boldsymbol{H}^1(\Omega), \varphi \in H^1(\Omega)$. It is well known that the bilinear form $b(\cdot,\cdot)$ satisfies the inf-sup condition

$$\sup_{\boldsymbol{v}\in\boldsymbol{H}_0^1(\Omega)\setminus\{\boldsymbol{0}\}} \frac{b(\boldsymbol{v}, q)}{\|\boldsymbol{v}\|_{1,\Omega}} \ge \zeta\|q\|_{0,\Omega} \quad \text{for all } q \in L_0^2(\Omega).$$

For $\boldsymbol{v} \in \boldsymbol{W}^{1,\infty}(\Omega)$ and $\varphi \in W^{1,\infty}(\Omega)$, one can show that there exists a constant $C_\infty > 0$ with $\|\boldsymbol{v}\|_{1,\Omega} \le C_\infty\|\boldsymbol{v}\|_{\boldsymbol{W}^{1,\infty}(\Omega)}$ and $\|\varphi\|_{1,\Omega} \le C_\infty\|\varphi\|_{W^{1,\infty}(\Omega)}$. The previous results imply the following lemma (see [12, Lemma 1.1]).

**Lemma 1.1** (Stability). *If $\boldsymbol{g} \in L^\infty(0, t_{\text{end}}; \boldsymbol{L}^\infty(\Omega))$, $\boldsymbol{u}_0 \in \boldsymbol{L}^2(\Omega)$ and $s_0, c_0 \in L^2(\Omega)$, then, for any solution $\boldsymbol{u}, s, c$ of (1.2) and for $t \in (0, t_{\text{end}}]$, there exists a constant $\gamma > 0$ such that*

$$\|\boldsymbol{u}\|_{L^2(0,t;\boldsymbol{H}^1(\Omega))} + \|s\|_{L^2(0,t;H^1(\Omega))} + \|c\|_{L^2(0,t;H^1(\Omega))} \le \gamma\big(\|\boldsymbol{u}_0\|_{0,\Omega} + \|s_0\|_{0,\Omega} + \|c_0\|_{0,\Omega}\big),$$

*where $\gamma$ might depend on $\eta_1$, $\tau$, $\mathrm{Sc}$, $\rho$, $\rho_{\mathrm{m}}$, $C_p$, $\|\boldsymbol{g}\|_{\infty,\Omega}$, $\alpha$, $\beta$, and $t$.*

# 2 | FINITE ELEMENT DISCRETIZATION AND A PRIORI ERROR BOUNDS

## 2.1 | Preliminaries and Galerkin method

We discretize $\Omega \subset \mathbb{R}^d$ by a family $\mathcal{T}_h$ of regular partitions into simplices $K$ (triangles in 2D or tetrahedra in 3D) of diameter $h_K$. We label by $K^-$ and $K^+$ the two elements adjacent to a facet $e$ (an edge in 2D or a face in 3D), while $h_e$ stands for the maximum diameter of $e$. Let $\mathcal{E}_h$ denote the set of all facets and $\mathcal{E}_h = \mathcal{E}_h^i \cup \mathcal{E}_h^\partial$ where $\mathcal{E}_h^i$ and $\mathcal{E}_h^\partial$ are the subset of interior facets and boundary facets, respectively. If $\boldsymbol{v}$ and $w$ are smooth vector and scalar fields defined on $\mathcal{T}_h$, then $(\boldsymbol{v}^\pm, w^\pm)$ denote the traces of $(\boldsymbol{v}, w)$ on $e$ that are the extensions from the interior of $K^+$ and $K^-$, respectively. Let $\boldsymbol{n}_e^+, \boldsymbol{n}_e^-$ be the outward unit normal vectors on the boundaries of two neighboring elements, $K^+$ and $K^-$, sharing $e$. We also use the notation $(\boldsymbol{w}_e \cdot \boldsymbol{n}_e)|_e = (\boldsymbol{w}^+ \cdot \boldsymbol{n}_e^+)|_e$, $\{\boldsymbol{v}\} := (\boldsymbol{v}^- + \boldsymbol{v}^+)/2$, $\{w\} := (w^- + w^+)/2$, $[\![\boldsymbol{v}]\!] := (\boldsymbol{v}^- - \boldsymbol{v}^+)$, and $[\![w]\!] := (w^- - w^+)$. For boundary jumps and averages, $\{\boldsymbol{v}\} = [\![\boldsymbol{v}]\!] = \boldsymbol{v}$ and $\{w\} = [\![w]\!] = w$. Finally, $\nabla_h$ denotes the broken gradient operator.

For $k \ge 1$ and a mesh $\mathcal{T}_h$ on $\Omega$, let us consider the finite-dimensional discrete spaces (see e.g. [11])

$$\begin{aligned} \boldsymbol{V}_h &:= \big\{\boldsymbol{v}_h \in \boldsymbol{H}(\operatorname{div}; \Omega) : \boldsymbol{v}_h|_K \in [\mathcal{P}_k(K)]^{\mathrm{d}} \quad \forall K \in \mathcal{T}_h; \quad \boldsymbol{v}_h \cdot \boldsymbol{n}_{\partial\Omega} = 0 \text{ on } \partial\Omega\big\}, \\ \boldsymbol{V}_h^t &:= \big\{\boldsymbol{v}_h \in \boldsymbol{L}^2(0, t_{\text{end}}; \boldsymbol{V}_h) : \partial_t \boldsymbol{v}_h \in \boldsymbol{L}^2(0, t_{\text{end}}; \boldsymbol{V}_h)\big\}, \\ \mathcal{Q}_h &:= \big\{q_h \in L_0^2(\Omega) : q_h|_K \in \mathcal{P}_{k-1}(K) \quad \forall K \in \mathcal{T}_h\big\}, \qquad \mathcal{Q}_h^t := L^2(0, t_{\text{end}}; \mathcal{Q}_h), \\ \mathcal{M}_h &:= \big\{s_h \in C(\bar{\Omega}) : s_h|_K \in \mathcal{P}_k(K) \quad \forall K \in \mathcal{T}_h\big\}, \qquad \mathcal{M}_{h,0} := \mathcal{M}_h \cap H_0^1(\Omega), \\ \mathcal{M}_{h,0}^t &:= \big\{s_h \in L^2(0, t_{\text{end}}; \mathcal{M}_{h,0}) : \partial_t s_h \in L^2(0, t_{\text{end}}; \mathcal{M}_{h,0})\big\}, \end{aligned}$$

which, in particular, satisfy div $\boldsymbol{V}_h \subset \mathcal{Q}_h$ (cf. [22]). Here $\mathcal{P}_k(K)$ denotes the local space spanned by polynomials of degree up to $k$ and $\boldsymbol{V}_h$ is the space of divergence-conforming BDM elements. Associated with these spaces, we state the following semi-discrete Galerkin formulation for problem (1.2): Find $(\boldsymbol{u}_h, p_h, s_h, c_h) \in \boldsymbol{V}_h^t \times \mathcal{Q}_h^t \times \mathcal{M}_{h,0}^t \times \mathcal{M}_{h,0}^t$ such that

$$
\begin{aligned}
&(\partial_t \boldsymbol{u}_h, \boldsymbol{v}_h)_\Omega + a_1^h(c_h; \boldsymbol{u}_h, \boldsymbol{v}_h) + c_1^h(\boldsymbol{u}_h; \boldsymbol{u}_h, \boldsymbol{v}_h) + b(\boldsymbol{v}_h, p_h) = F(s_h, c_h, \boldsymbol{v}_h) \quad \forall \boldsymbol{v}_h \in \boldsymbol{V}_h,\\
&b(\boldsymbol{u}_h, q_h) = 0 \quad \forall q_h \in \mathcal{Q}_h, \quad (\partial_t s_h, \varphi_h)_\Omega + a_2(s_h, \varphi_h) + c_2(\boldsymbol{u}_h; s_h, \varphi_h) = 0 \quad \forall \varphi_h \in \mathcal{M}_{h,0},\\
&(\partial_t c_h, \psi_h)_\Omega + (1/\tau) a_2(c_h, \psi_h) + c_2(\boldsymbol{u}_h - v_{\mathrm{p}} \boldsymbol{e}_z; c_h, \psi_h) = 0 \quad \forall \psi_h \in \mathcal{M}_{h,0}.
\end{aligned} \tag{2.1}
$$

The discrete versions of the variational forms $a_1^h(\cdot;\cdot,\cdot)$ and $c_1^h(\cdot;\cdot,\cdot)$ are defined using a symmetric interior penalty and an upwind approach, respectively (see, e.g., [7, 22]), where $a_0 > 0$ is a jump penalization parameter:

$$
\begin{aligned}
a_1^h(c_h; \boldsymbol{u}_h, \boldsymbol{v}_h) &:= \int_\Omega \nu(c_h) \boldsymbol{\nabla}_h(\boldsymbol{u}_h) : \boldsymbol{\nabla}_h(\boldsymbol{v}_h)\, \mathrm{d}\boldsymbol{x} + \sum_{e \in \mathcal{E}_h} \int_e \Big( -\{\nu(c_h) \boldsymbol{\nabla}_h(\boldsymbol{u}_h) \boldsymbol{n}_e\} \cdot [\![\boldsymbol{v}_h]\!] \\
&\qquad - \{\nu(c_h) \boldsymbol{\nabla}_h(\boldsymbol{v}_h) \boldsymbol{n}_e\} \cdot [\![\boldsymbol{u}_h]\!] + \frac{a_0}{h_e} \nu(c_h) [\![\boldsymbol{u}_h]\!] \cdot [\![\boldsymbol{v}_h]\!] \Big)\, \mathrm{d}S, \qquad (2.2)\\
c_1^h(\boldsymbol{w}_h; \boldsymbol{u}_h, \boldsymbol{v}_h) &:= \int_\Omega (\boldsymbol{w}_h \cdot \nabla) \boldsymbol{u}_h \cdot \boldsymbol{v}_h\, \mathrm{d}\boldsymbol{x} + \sum_{e \in \mathcal{E}_h^i} \int_e \Big( (\boldsymbol{w}_e \cdot \boldsymbol{n}_e) [\![\boldsymbol{u}_h]\!] \cdot \{\boldsymbol{v}_h\} + \frac{1}{2} |\boldsymbol{w}_e \cdot \boldsymbol{n}_e| [\![\boldsymbol{u}_h]\!] \cdot [\![\boldsymbol{v}_h]\!] \Big) \mathrm{d}S.
\end{aligned}
$$

We partition the interval $[0, t_{\mathrm{end}}]$ into $N$ subintervals $[t_{n-1}, t_n]$ of length $\Delta t$. We use the implicit BDF2 scheme where all first-order time derivatives are approximated using the centered operator

$$
\partial_t \boldsymbol{u}_h(t^{n+1}) \approx (1/(2\Delta t)) \mathcal{D} \boldsymbol{u}_h^{n+1}, \quad \text{where} \quad \mathcal{D} y^{n+1} := 3y^{n+1} - 4y^n + y^{n-1}, \tag{2.3}
$$

and for the first time step a first-order backward Euler method is used (not detailed here; see [12, Section 2.2]). The resulting set of nonlinear equations is solved by an iterative Newton–Raphson method with exact Jacobian. Hence for $1 \le n \le N-1$, the complete discrete system is given by

$$
\begin{aligned}
&\frac{1}{3} \big( \mathcal{D} \boldsymbol{u}_h^{n+1}, \boldsymbol{v}_h \big)_\Omega = \frac{2}{3} \Delta t \big( -a_1^h(c_h^{n+1}; \boldsymbol{u}_h^{n+1}, \boldsymbol{v}_h) - c_1^h(\boldsymbol{u}_h^{n+1}; \boldsymbol{u}_h^{n+1}, \boldsymbol{v}_h) - b(\boldsymbol{v}_h, p_h^{n+1}) + F(s_h^{n+1}, c_h^{n+1}, \boldsymbol{v}_h) \big)\\
&\qquad\qquad \forall \boldsymbol{v}_h \in \boldsymbol{V}_h,\\
&b(\boldsymbol{u}_h^{n+1}, q_h) = 0 \quad \forall q_h \in \mathcal{Q}_h,\\
&\frac{1}{3} \big( \mathcal{D} s_h^{n+1}, \varphi_h \big)_\Omega = \frac{2}{3} \Delta t \big( -a_2(s_h^{n+1}, \varphi_h) - c_2(\boldsymbol{u}_h^{n+1}; s_h^{n+1}, \varphi_h) \big) \quad \forall \varphi_h \in \mathcal{M}_{h,0},\\
&\frac{1}{3} \big( \mathcal{D} c_h^{n+1}, \psi_h \big)_\Omega = \frac{2}{3} \Delta t \Big( -\frac{1}{\tau} a_2(c_h^{n+1}, \psi_h) - c_2(\boldsymbol{u}_h^{n+1} - v_{\mathrm{p}} \boldsymbol{e}_z; c_h^{n+1}, \psi_h) \Big) \quad \forall \psi_h \in \mathcal{M}_{h,0}.
\end{aligned} \tag{2.4}
$$

## 2.2 | Properties of the discrete problem

We introduce for $r \ge 0$ the broken $\boldsymbol{H}^r$ space $\boldsymbol{H}^r(\mathcal{T}_h) := \{\boldsymbol{v} \in \boldsymbol{L}^2(\Omega) : \boldsymbol{v}|_K \in \boldsymbol{H}^r(K),\ K \in \mathcal{T}_h\}$ as well as the mesh-dependent broken norms

$$
\|\boldsymbol{v}\|_{*,\mathcal{T}_h}^2 := \sum_{K \in \mathcal{T}_h} \|\boldsymbol{\nabla}_h(\boldsymbol{v})\|_{\boldsymbol{L}^2(K)}^2 + \sum_{e \in \mathcal{E}_h} \frac{1}{h_e} \|[\![\boldsymbol{v}]\!]\|_{\boldsymbol{L}^2(e)}^2,
$$

$$
\|\boldsymbol{v}\|_{1,\mathcal{T}_h}^2 := \|\boldsymbol{v}\|_{\boldsymbol{L}^2(\Omega)}^2 + \|\boldsymbol{v}\|_{*,\mathcal{T}_h}^2 \quad \forall \boldsymbol{v} \in \boldsymbol{H}^1(\mathcal{T}_h), \quad \|\boldsymbol{v}\|_{2,\mathcal{T}_h}^2 := \|\boldsymbol{v}\|_{1,\mathcal{T}_h}^2 + \sum_{K \in \mathcal{T}_h} h_K^2 |\boldsymbol{v}|_{H^2(K)}^2 \quad \forall \boldsymbol{v} \in \boldsymbol{H}^2(\mathcal{T}_h),
$$

where the stronger norm $\|\cdot\|_{2,\mathcal{T}_h}$ is used to show continuity. From the inverse estimate $|\boldsymbol{w}|_{2,K} \le Ch_K^{-1}|\boldsymbol{w}|_{1,K}$ for all $K \in \mathcal{T}_h$, $\boldsymbol{w} \in [\mathcal{P}_k(K)]^d$ it can be seen that this norm is equivalent to $\|\cdot\|_{1,\mathcal{T}_h}$ on $\boldsymbol{V}_h$ (cf. [7]). Finally, adapting the argument of [21, Proposition 4.5], we get the following version of the discrete Sobolev embedding: for $r = 2, 4$ there exists a constant $C_{\text{emb}} > 0$ with

$$\|\boldsymbol{v}\|_{L^r(\Omega)} \le C_{\text{emb}}\|\boldsymbol{v}\|_{1,\mathcal{T}_h} \quad \forall \boldsymbol{v} \in \boldsymbol{H}^1(\mathcal{T}_h). \tag{2.5}$$

With these norms, we can prove continuity of the trilinear and bilinear forms of the variational formulation, see [7, Section 4].

**Lemma 2.1.** *The following properties hold:* $|a_1^h(\cdot, \boldsymbol{u}, \boldsymbol{v})| \le C\|\boldsymbol{u}\|_{2,\mathcal{T}_h}\|\boldsymbol{v}\|_{1,\mathcal{T}_h}$ *for all* $\boldsymbol{u} \in \boldsymbol{H}^2(\mathcal{T}_h)$, $\boldsymbol{v} \in \boldsymbol{V}_h$, $|a_1^h(\cdot, \boldsymbol{u}, \boldsymbol{v})| \le \tilde{C}_a\|\boldsymbol{u}\|_{1,\mathcal{T}_h}\|\boldsymbol{v}\|_{1,\mathcal{T}_h}$ *for all* $\boldsymbol{u}, \boldsymbol{v} \in \boldsymbol{V}_h$, *and* $|b(\boldsymbol{v}, q)| \le \tilde{C}_b\|\boldsymbol{v}\|_{1,\mathcal{T}_h}\|q\|_{0,\Omega}$ *for all* $\boldsymbol{v} \in \boldsymbol{H}^1(\mathcal{T}_h)$, $q \in L^2(\Omega)$. *Moreover, for all* $\boldsymbol{w} \in \boldsymbol{H}^1(\mathcal{T}_h)$ *and* $\varphi, \psi \in H^1(\Omega)$, *there holds* $|c_2(\boldsymbol{w}; \varphi, \psi)| \le \tilde{C}\|\boldsymbol{w}\|_{1,\mathcal{T}_h}\|\varphi\|_{1,\Omega}\|\psi\|_{1,\Omega}$.

Moreover, for $\gamma_1, \gamma_2 \in H^1(\Omega)$, $\boldsymbol{u} \in \boldsymbol{C}^1(\mathcal{T}_h) \cap \boldsymbol{H}_0^1(\Omega)$ and $\boldsymbol{v} \in \boldsymbol{V}_h$, there holds

$$|a_1^h(\gamma_1; \boldsymbol{u}, \boldsymbol{v}) - a_1^h(\gamma_2; \boldsymbol{u}, \boldsymbol{v})| \le \tilde{C}_{\text{Lip}}\|\gamma_1 - \gamma_2\|_{1,\Omega}\|\boldsymbol{u}\|_{\boldsymbol{W}^{1,\infty}(\mathcal{T}_h)}\|\boldsymbol{v}\|_{1,\mathcal{T}_h}, \tag{2.6}$$

where the constant $\tilde{C}_{\text{Lip}} > 0$ is independent of $h$ (cf. [13]).

Let $\boldsymbol{w} \in \boldsymbol{H}_0(\text{div}^0; \Omega)$ and let us introduce the jump seminorm

$$|\boldsymbol{u}_h|_{\boldsymbol{w},\text{upw}} := \sum_{e \in \mathcal{E}_h^i} \int_e \frac{1}{2}|\boldsymbol{w}_e \cdot \boldsymbol{n}_e||[\![\boldsymbol{u}_h]\!]|^2 \, \mathrm{d}S.$$

Then, due to the skew-symmetric form of the operators $c_1^h$ and $c_2$, and the positivity of the nonlinear upwind term of $c_1^h$, $c_1^h(\boldsymbol{w}; \boldsymbol{u}_h, \boldsymbol{u}_h) = |\boldsymbol{u}_h|^2_{\boldsymbol{w},\text{upw}} \ge 0$ for all $\boldsymbol{u}_h \in \boldsymbol{V}_h$ and $c_2(\boldsymbol{w}; \psi_h, \psi_h) = 0$ for all $\psi_h \in \mathcal{M}_h$. Moreover, we have the following relation, which is based on (2.5) and follows by the same method as in ref. [21]: for any $\boldsymbol{w}_1, \boldsymbol{w}_2, \boldsymbol{u} \in \boldsymbol{H}^2(\mathcal{T}_h)$ there holds

$$|c_1^h(\boldsymbol{w}_1; \boldsymbol{u}, \boldsymbol{v})| - |c_1^h(\boldsymbol{w}_2; \boldsymbol{u}, \boldsymbol{v})| \le \tilde{C}_c\|\boldsymbol{w}_1 - \boldsymbol{w}_2\|_{1,\mathcal{T}_h}\|\boldsymbol{v}\|_{1,\mathcal{T}_h}\|\boldsymbol{u}\|_{1,\mathcal{T}_h} \quad \forall \boldsymbol{v} \in \boldsymbol{V}_h. \tag{2.7}$$

We also have $F(\psi, \phi, \boldsymbol{v}) \le C_f(\|\psi\|_{0,\Omega} + \|\phi\|_{0,\Omega})\|\boldsymbol{v}\|_{0,\Omega}$ for all $\boldsymbol{v} \in \boldsymbol{V}_h$.

Finally, we recall from ref. [22] the following discrete inf-sup condition for $b(\cdot,\cdot)$, where $\tilde{\xi}$ is independent of $h$:

$$\sup_{\boldsymbol{v}_h \in \boldsymbol{V}_h \setminus \{\boldsymbol{0}\}} \frac{b(\boldsymbol{v}_h, q_h)}{\|\boldsymbol{v}_h\|_{1,\mathcal{T}_h}} \ge \tilde{\xi}\|q_h\|_{0,\Omega} \quad \forall q_h \in Q_h. \tag{2.8}$$

## 2.3 | Stability and solvability (existence of a discrete solution)

Applying the previous estimates we may prove the following theorem (see ref. [12] for details).

**Theorem 2.2.** *If* $(\boldsymbol{u}_h^{n+1}, p_h^{n+1}, s_h^{n+1}, c_h^{n+1}) \in \boldsymbol{V}_h \times Q_h \times (\mathcal{M}_{h,0})^2$ *is a solution of (2.4) with initial data* $(\boldsymbol{u}_h^1, s_h^1, c_h^1)$ *and* $(\boldsymbol{u}_h^0, s_h^0, c_h^0)$, *then the following bounds (plus an analogous inequality for* $c_h$*) hold, where* $C_1$, $C_2$ *are independent of* $h$ *and* $\Delta t$*:*

$$\begin{aligned}
&\|\boldsymbol{u}_h^{n+1}\|^2_{0,\Omega} + \|2\boldsymbol{u}_h^{n+1} - \boldsymbol{u}_h^n\|^2_{0,\Omega} + \sum_{j=1}^n \|\Lambda\boldsymbol{u}_h^j\|^2_{0,\Omega} + \sum_{j=1}^n \Delta t\|\boldsymbol{u}_h^{j+1}\|^2_{1,\mathcal{T}_h} + \sum_{j=1}^n \Delta t|\boldsymbol{u}_h^j|^2_{\boldsymbol{u}_h^j,\text{upw}} \\
&\quad \le C_1\big(\|s_h^1\|^2_{0,\Omega} + \|2s_h^1 - s_h^0\|^2_{0,\Omega} + \|c_h^1\|^2_{0,\Omega} + \|2c_h^1 - c_h^0\|^2_{0,\Omega} + \|\boldsymbol{u}_h^1\|^2_{0,\Omega} + \|2\boldsymbol{u}_h^1 - \boldsymbol{u}_h^0\|^2_{0,\Omega}\big),
\end{aligned} \tag{2.9}$$

$$\|s_h^{n+1}\|^2_{0,\Omega} + \|2s_h^{n+1} - s_h^n\|^2_{0,\Omega} + \sum_{j=1}^n \|\Lambda s_h^j\|^2_{0,\Omega} + \sum_{j=1}^n \Delta t\|s_h^{j+1}\|^2_{1,\Omega} \le C_2\big(\|s_h^1\|^2_{0,\Omega} + \|2s_h^1 - s_h^0\|^2_{0,\Omega}\big).$$

Note that, in contrast to the linear case, the stability result and the existence of a discrete solution do not guarantee, in general, uniqueness of solution.

**Theorem 2.3** (Existence of a discrete solution). *Assume that* $\min\{\tilde{\alpha}_a, \tilde{\alpha}_a/\tau\} > C_f^2/(2\tilde{\alpha}_a)$. *Then problem (2.4), with initial data* $(\boldsymbol{u}_h^1, s_h^1, c_h^1)$ *and* $(\boldsymbol{u}_h^0, s_h^0, c_h^0)$ *(where* $(\boldsymbol{u}_h^1, s_h^1, c_h^1)$ *is obtained from* $(\boldsymbol{u}_h^0, s_h^0, c_h^0)$ *by a backward Euler method), admits a (not necessarily unique) solution* $(\boldsymbol{u}_h^{n+1}, p_h^{n+1}, s_h^{n+1}, c_h^{n+1}) \in \boldsymbol{V}_h \times \mathcal{Q}_h \times \mathcal{M}_{h,0} \times \mathcal{M}_{h,0}$.

The proof of Theorem 2.3 is conducted in ref. [12] using a fixed-point argument that employs Brouwer's fixed-point theorem in the form given by ref. [20, Corollary 1.1, Chapter IV].

## 2.4 | A priori error estimates

The results summarized in this section follow from standard arguments applicable to the approximation and error bounds for isolated solutions. For this we require to assume the uniqueness of discrete solution. Let us then denote by $\mathcal{I}_h : H^2(\Omega) \to \mathcal{M}_h$ the nodal interpolator with respect to a unisolvent set of Lagrangian interpolation nodes associated with $\mathcal{M}_h$. Furthermore, $\Pi_h \boldsymbol{u}$ denotes the BDM projection of $\boldsymbol{u}$, and $\mathcal{L}_h p$ is the $L^2$-projection of $p$ onto $\mathcal{Q}_h$. Under usual assumptions, the following approximation properties hold (see ref. [22]):

$$\begin{aligned} &\|\boldsymbol{u} - \Pi_h \boldsymbol{u}\|_{1,\mathcal{T}_h} \le C^* h^k \|\boldsymbol{u}\|_{k+1,\Omega}, \quad \|c - \mathcal{I}_h c\|_{1,\Omega} \le C^* h^k \|c\|_{k+1,\Omega}, \\ &\|s - \mathcal{I}_h s\|_{1,\Omega} \le C^* h^k \|s\|_{k+1,\Omega}, \quad \|p - \mathcal{L}_h p\|_{0,\Omega} \le C^* h^k \|p\|_{k,\Omega}. \end{aligned} \tag{2.10}$$

The following development follows the structure adopted in ref. [2]. We begin with a property of the discrete bilinear forms and the continuous variational formulation.

**Lemma 2.4.** *Assume that* $\boldsymbol{u} \in \boldsymbol{L}^2(0, t_{\text{end}}; \boldsymbol{H}^2(\Omega))$, $\partial_t \boldsymbol{u} \in \boldsymbol{L}^2(0, t_{\text{end}}; \boldsymbol{L}^2(\Omega))$, $p \in Q^t$ *and* $s, c \in M^t$. *Then for a.e* $t \in [0, t_{\text{end}}]$, *we have*

$$(\partial_t \boldsymbol{u}, \boldsymbol{v})_\Omega + a_1^h(c; \boldsymbol{u}, \boldsymbol{v}) + c_1^h(\boldsymbol{u}; \boldsymbol{u}, \boldsymbol{v}) + b(\boldsymbol{v}, p) = F(s, c, \boldsymbol{v}) \quad \forall \boldsymbol{v} \in \boldsymbol{V}_h, \quad b(\boldsymbol{u}, q) = 0 \quad \forall q \in \mathcal{Q}_h,$$

$$(\partial_t s, \varphi)_\Omega + a_2(s, \varphi) + c_2(\boldsymbol{u}; s, \varphi) = 0, \quad (\partial_t c, \psi)_\Omega + \frac{1}{\tau} a_2(c, \psi) + c_2(\boldsymbol{u} - v_{\mathrm{p}} \boldsymbol{e}_z; c, \psi) = 0 \quad \forall \varphi, \psi \in \mathcal{M}_{h,0}.$$

*Proof.* Since we have assumed that $\boldsymbol{u} \in \boldsymbol{H}^2(\Omega)$, integration by parts yields the required result. See also ref. [7]. The third and fourth equations are a straightforward consequence of properties of the continuous weak form. □

Since for the following theorems we will assume the exact $c$ and $s$ belong to $H^2(\Omega)$, we have $c$, $s \in C(\bar{\Omega})$. Now we decompose the errors as follows:

$$\begin{aligned} &\boldsymbol{u} - \boldsymbol{u}_h = E_{\boldsymbol{u}} + \xi_{\boldsymbol{u}} = (\boldsymbol{u} - \Pi_h \boldsymbol{u}) + (\Pi_h \boldsymbol{u} - \boldsymbol{u}_h), \quad p - p_h = E_p + \xi_p = (p - \mathcal{L}_h p) + (\mathcal{L}_h p - p_h), \\ &s - s_h = E_s + \xi_s = (s - \mathcal{I}_h s) + (\mathcal{I}_h s - s_h), \quad c - c_h = E_c + \xi_c = (c - \mathcal{I}_h c) + (\mathcal{I}_h c - c_h). \end{aligned}$$

Assuming that $\boldsymbol{u}_h^0 = \Pi_h \boldsymbol{u}(0)$, $s_h^0 = \mathcal{I}_h s(0)$ and $c_h^0 = \mathcal{I}_h c(0)$, we also use the notation $E_{\boldsymbol{u}}^n = (\boldsymbol{u}(t_n) - \Pi_h \boldsymbol{u}(t_n))$ and $\xi_{\boldsymbol{u}}^n = (\Pi_h \boldsymbol{u}(t_n) - \boldsymbol{u}_h^n)$, and similar notation for other variables. Since for the first time iteration of system (2.1) we adopt a backward Euler scheme, a dedicated error estimate is required for this step.

For brevity, in the following two theorems we do not precisely state the regularity assumptions on $\boldsymbol{u}$ and its time derivatives, $p$, $s$, and $c$, but refer to Theorems 2.4 and 2.5 in ref. [12] for details.

**Theorem 2.5.** *Let* $(\boldsymbol{u}, p, s, c)$ *be the unique solution of (1.2) under the assumptions of Section 1.3, and* $(\boldsymbol{u}_h, p_h, s_h, c_h)$ *be a solution of (2.4). There exist positive constants* $C_u^1$, $C_s^1$, $C_c^1$, *independently of h and* $\Delta t$, *such that, for* $\phi = c, s$,

$$\frac{\|\xi_{\boldsymbol{u}}^1\|_{0,\Omega}^2}{4} + \frac{\Delta t}{2} \tilde{\alpha}_a \|\xi_{\boldsymbol{u}}\|_{1,\mathcal{T}_h}^2 + \Delta t |\xi_{\boldsymbol{u}}^1|_{\boldsymbol{u}_h^1,\text{upw}}^2 \le C_u^1 (h^{2k} + \Delta t^4), \quad \frac{\|\xi_\phi^1\|_{0,\Omega}^2}{4} + \frac{\Delta t}{2} \tilde{\alpha}_a \|\xi_\phi\|_{1,\Omega}^2 \le C_\phi^1 (h^{2k} + \Delta t^4).$$

**Theorem 2.6.** *Under certain additional regularity assumptions on $\boldsymbol{u}$ and its time derivatives of up to third-order there exist constants $C, \gamma_1 > 0$, independent of $h$ and $\Delta t$, such that, for all $m+1 \leq N$,*

$$\|\xi_{\boldsymbol{u}}^{m+1}\|_{0,\Omega}^2 + \|2\xi_{\boldsymbol{u}}^{m+1} - \xi_{\boldsymbol{u}}^m\|_{0,\Omega}^2 + \sum_{n=1}^{m} \|\Lambda \xi_{\boldsymbol{u}}^n\|_{0,\Omega}^2 + \sum_{n=1}^{m} \Delta t \tilde{\alpha}_a \|\xi_{\boldsymbol{u}}^{n+1}\|_{1,\mathcal{T}_h}^2 + \sum_{n=1}^{m} \Delta t |\xi_{\boldsymbol{u}}^{n+1}|_{\boldsymbol{u}_h^{n+1},\mathrm{upw}}^2$$
$$\leq C(\Delta t^4 + h^{2k}) + \sum_{n=1}^{m} \gamma_1 \Delta t \|\xi_c^{n+1}\|_{1,\Omega}^2.$$

Note that Theorems 2.5 and 2.6 require a smallness assumption on the velocity solution of the continuous problem. The assumption is needed due to the coupling through the viscosity with the balance equation of concentration. If such dependency is removed, for instance when a constant viscosity value is used, the smallness assumption is no longer required. Theorems similar to Theorem 2.6 also hold for $\xi_s$ and $\xi_c$ in place of $\xi_u$ but are not written out here, see ref. [12, Theorems 2.6, Theorem 2.7].

**Theorem 2.7.** *Under the same assumptions of Theorem 2.6 (and its versions for $\xi_s$ and $\xi_c$) there exist positive constants $\gamma_u$, $\gamma_s$ and $\gamma_c$ independent of $\Delta t$ and $h$, such that, for a sufficiently small $\Delta t$ and all $m+1 \leq N$, there hold*

$$\left( \|\xi_{\boldsymbol{u}}^{m+1}\|_{0,\Omega}^2 + \|2\xi_{\boldsymbol{u}}^{m+1} - \xi_{\boldsymbol{u}}^m\|_{0,\Omega}^2 + \sum_{n=1}^{m} \left( \|\Lambda \xi_{\boldsymbol{u}}^n\|_{0,\Omega}^2 + \Delta t \tilde{\alpha}_a \|\xi_{\boldsymbol{u}}^{n+1}\|_{1,\mathcal{T}_h}^2 + \Delta t |\xi_{\boldsymbol{u}}^{n+1}|_{\boldsymbol{u}_h^{n+1},\mathrm{upw}}^2 \right) \right)^{1/2} \leq \gamma_u(\Delta t^2 + h^k),$$

$$\left( \|\xi_s^{m+1}\|_{0,\Omega}^2 + \|2\xi_s^{m+1} - \xi_s^m\|_{0,\Omega}^2 + \sum_{n=1}^{m} \left( \|\Lambda \xi_s^n\|_{0,\Omega}^2 + \Delta t \hat{\alpha}_a \|\xi_s^{n+1}\|_{1,\Omega}^2 \right) \right)^{1/2} \leq \gamma_s(\Delta t^2 + h^k),$$

*and the same inequality with $s$ replaced by $c$. Moreover, if $p \in L^\infty(0, t_{\mathrm{end}}; H^2(\Omega))$, we have*

$$\left( \sum_{n=1}^{m} \Delta t \|p(t_{n+1}) - p_h^{n+1}\|_{0,\Omega}^2 \right)^{1/2} \leq \hat{\gamma}_p(\Delta t^2 + h^k).$$

## 3 | A POSTERIORI ERROR ANALYSIS

We next proceed to derive and analyze a posteriori error estimators. We split the presentation into three cases of increasing complexity, starting with an estimator focusing on the steady coupled problem. To outline the three steps (of increasing complexity) of the a posteriori error analysis in ref.[12], we first consider the following coupled problem in weak form that is a stationary version of (1.2): find $(\boldsymbol{u}, p, s, c) \in \boldsymbol{H}_0^1 \times L_0^2 \times H_0^1 \times H_0^1$ such that

$$\begin{aligned} &a_1(c, \boldsymbol{u}, \boldsymbol{v}) + c_1(\boldsymbol{u}; \boldsymbol{u}, \boldsymbol{v}) + b(\boldsymbol{v}, p) = (\boldsymbol{f}, \boldsymbol{v})_{0,\Omega}, \quad b(\boldsymbol{u}, q) = 0, \\ &a_2(s, \phi) + c_2(\boldsymbol{u}; s, \phi) = (f_1, \phi)_{0,\Omega}, \quad (1/\tau) a_2(c, \psi) + c_2(\boldsymbol{u} - v_p \boldsymbol{e}_z; c, \psi) = (f_2, \psi)_{0,\Omega} \end{aligned} \tag{3.1}$$

for all $\boldsymbol{v} \in \boldsymbol{H}_0^1(\Omega)$, $q \in L_0^2(\Omega)$, $\phi \in H_0^1(\Omega)$, and $\psi \in H_0^1(\Omega)$, respectively, where $(\alpha s + \beta c)\boldsymbol{g} = (\rho/\rho_{\mathrm{m}})\boldsymbol{g} = \boldsymbol{f} \in \boldsymbol{L}^2(\Omega)$, and $f_1, f_2$ are taken as constant. The discrete counterpart of this problem can be formulated as follows: find $(\boldsymbol{u}_h, p_h, s_h, c_h) \in \boldsymbol{V}_h \times \mathcal{Q}_h \times \mathcal{M}_{h,0} \times \mathcal{M}_{h,0}$ such that for all $\boldsymbol{v} \in \boldsymbol{V}_h$, $q \in \mathcal{Q}_h$, $\phi \in \mathcal{M}_{h,0}$ and $\psi \in \mathcal{M}_{h,0}$, respectively,

$$\begin{aligned} &a_1(c_h, \boldsymbol{u}_h, \boldsymbol{v}) + c_1(\boldsymbol{u}_h; \boldsymbol{u}_h, \boldsymbol{v}) + b(\boldsymbol{v}, p) = (\boldsymbol{f}_h, \boldsymbol{v})_{0,\Omega}, \quad b(\boldsymbol{u}_h, q) = 0, \\ &a_2(s_h, \phi) + c_2(\boldsymbol{u}_h; s_h, \phi) = (f_1, \phi)_{0,\Omega}, \quad (1/\tau) a_2(c_h, \psi) + c_2(\boldsymbol{u}_h - v_p \boldsymbol{e}_z; c_h, \psi) = (f_2, \psi)_{0,\Omega}. \end{aligned} \tag{3.2}$$

The a posteriori error estimator is based in the computation of the following element-wise and facet-wise residuals:

$$\boldsymbol{R}_K := \{\boldsymbol{f}_h + \mathbf{div}(\nu(c_h)\boldsymbol{\nabla}\boldsymbol{u}_h) - \boldsymbol{u}_h \cdot \boldsymbol{\nabla}\boldsymbol{u}_h - (\rho_{\mathrm{m}})^{-1}\nabla p_h\}|_K,$$

$$R_{1,K} := \{f_1 + \mathrm{Sc}^{-1}\Delta s_h - \boldsymbol{u}_h \cdot \nabla s_h\}|_K, \quad R_{2,K} := \{f_2 + (\tau\mathrm{Sc})^{-1}\Delta c_h - (\boldsymbol{u}_h - v_p\boldsymbol{e}_z)\cdot\nabla c_h\}|_K, \tag{3.3}$$

$$\boldsymbol{R}_e := \frac{1}{2}[\![\frac{p_h}{\rho_{\mathrm{m}}}\boldsymbol{I} - \nu(c_h)\boldsymbol{\nabla u}_h)\boldsymbol{n}]\!], \quad R_{1,e} := \frac{1}{2\mathrm{Sc}}[\![(\nabla s_h)\cdot\boldsymbol{n}]\!], \quad R_{2,e} := [\![((\tau\mathrm{Sc})^{-1}\nabla c_h)\cdot\boldsymbol{n}]\!] \quad \text{for } e \in \mathcal{E}_h \setminus \Gamma$$

and $\boldsymbol{R}_e = R_{1,e} = R_{2,e} := 0$ for $e \in \Gamma$. The corresponding element-wise error estimator is then

$$\Psi_K^2 := \Psi_{R_K}^2 + \Psi_{e_K}^2 + \Psi_{J_K}^2, \quad \text{where} \quad \Psi_{R_K}^2 := h_K^2\big(\|\boldsymbol{R}_K\|_{0,K}^2 + \|R_{1,K}\|_{0,K}^2 + \|R_{2,K}\|_{0,K}^2\big),$$

$$\Psi_{e_K}^2 := \sum_{e\in\partial K} h_e\big(\|\boldsymbol{R}_e\|_{0,e}^2 + \|R_{1,e}\|_{0,e}^2 + \|R_{2,e}\|_{0,e}^2\big), \quad \Psi_{J_K}^2 := \sum_{e\in\partial K}\frac{1}{h_e}\|[\![\boldsymbol{u}_h]\!]\|_{0,e}^2.$$

These quantities define the global a posteriori error estimator $\Psi := (\sum_{K\in\mathcal{T}_h}\Psi_K^2)^{1/2}$ for the nonlinear coupled steady problem (3.2), for which one can eventually prove that it is reliable and efficient [12]:

**Theorem 3.1** (Reliability). *Let $(\boldsymbol{u}, p, s, c)$ be the unique solution to (3.1) and $(\boldsymbol{u}_h, p_h, s_h, c_h)$ a solution to (3.2). Let $|||(\boldsymbol{v}, q, \phi, \psi)|||^2 := \|\boldsymbol{v}\|_{1,\mathcal{T}_h}^2 + \|q\|_{0,\Omega}^2 + \|\phi\|_{1,\Omega}^2 + \|\psi\|_{1,\Omega}^2$. If $\|\boldsymbol{u}\|_{1,\infty} < M$, $\|s\|_\infty < M$ and $\|c\|_\infty < M$ for sufficiently small $M$, then $|||(\boldsymbol{u} - \boldsymbol{u}_h, p - p_h, s - s_h, c - c_h)||| \le C(\Psi + \|\boldsymbol{f} - \boldsymbol{f}_h\|_{0,\Omega})$, where $C > 0$ is a constant independent of $h$.*

**Theorem 3.2** (Efficiency). *Let $(\boldsymbol{u}, p, s, c)$ be the unique solution to (3.1) and $(\boldsymbol{u}_h, p_h, s_h, c_h)$ a solution of problem (3.2). Then there exists a constant $C > 0$ that is independent of $h$ such that*

$$\Psi \le C\left(|||(\boldsymbol{u} - u_h, p - p_h, s - s_h, c - c_h)||| + \left(\sum_{K\in\mathcal{T}_h} h_K^2\|\boldsymbol{f} - \boldsymbol{f}_h\|_{0,K}^2\right)^{1/2}\right).$$

Let us now turn to the transient problem, for which we utilize the following semi-discrete formulation, where $\partial_t\boldsymbol{u}_h, \partial_t s_h$, and $\partial_t c_h$ appear on the right-hand sides as in the so-called elliptic reconstruction approach (cf. [15]): find $(\tilde{\boldsymbol{u}}_h, \tilde{p}_h, \tilde{c}_h, \tilde{s}_h) \in C^{0,1}(0, t_{\mathrm{end}}; \boldsymbol{V}_h) \times C^{0,0}(0, t_{\mathrm{end}}; \mathcal{Q}_h) \times C^{0,1}(0, t_{\mathrm{end}}; \mathcal{M}_{h,0}) \times C^{0,1}(0, t_{\mathrm{end}}; \mathcal{M}_{h,0})$ such that

$$\begin{aligned} &a_1(c_h, \tilde{\boldsymbol{u}}_h, \boldsymbol{v}) + c_1(\boldsymbol{u}_h; \tilde{\boldsymbol{u}}_h, \boldsymbol{v}) + b(\boldsymbol{v}, \tilde{p}) = (\tilde{\boldsymbol{f}}, \boldsymbol{v}) \quad \forall \boldsymbol{v} \in \boldsymbol{V}_h, \quad b(\tilde{\boldsymbol{u}}_h, q) = 0 \quad \forall q \in \mathcal{Q}_h, \\ &a_2(\tilde{s}_h, \phi) + c_2(\boldsymbol{u}_h; \tilde{s}_h, \phi) = (f_1, \phi), \quad (1/\tau)a_2(\tilde{c}_h, \psi) + c_2(\boldsymbol{u}_h - v_p\boldsymbol{e}_z; \tilde{c}_h, \psi) = (f_2, \psi) \quad \forall \phi, \psi \in \mathcal{M}_{h,0}, \\ &\text{where} \quad \tilde{\boldsymbol{f}} = (\alpha s_h + \beta c_h)\mathbf{g} - \partial_t\boldsymbol{u}_h \in \boldsymbol{L}^2(\Omega), \quad f_1 = -\partial_t s_h \in L^2(\Omega), \quad f_2 = -\partial_t c_h \in L^2(\Omega). \end{aligned} \tag{3.4}$$

By (2.1), $(\boldsymbol{u}_h, p_h, c_h, s_h)$ is also a discrete solution of (3.4) for each $t \in (0, t_{\mathrm{end}}]$. But, since the discrete weak formulation (3.4) is well-posed, we also conclude that $(\tilde{\boldsymbol{u}}_h, \tilde{p}_h, \tilde{c}_h, \tilde{s}_h) = (\boldsymbol{u}_h, p_h, c_h, s_h)$ for each $t \in (0, t_{\mathrm{end}}]$. We may now define the following semi-discrete error indicator:

$$\begin{aligned} \Theta^2 &:= \|e_{\boldsymbol{u}}(0)\|_{0,\Omega}^2 + \|e_c(0)\|_{0,\Omega}^2 + \|e_s(0)\|_{0,\Omega}^2 + \int_0^{t_{\mathrm{end}}}\Psi^2\,\mathrm{d}t + \int_0^{t_{\mathrm{end}}}\Theta_2^2\,\mathrm{d}t + \max_{0\le t\le T}\Theta_3^2, \\ \Theta_2^2 &:= \sum_{e\in\mathcal{E}_h} h_e\|[\![\partial_t\boldsymbol{u}_h]\!]\|_{0,e}^2, \quad \Theta_3^2 := \sum_{e\in\mathcal{E}_h} h_e\|[\![\boldsymbol{u}_h]\!]\|_{0,e}^2, \end{aligned} \tag{3.5}$$

where $\Psi$ is the global a posteriori error estimator for the steady problem (3.3) and we now replace $\boldsymbol{f}$ and $f_1, f_2$ by $\tilde{\boldsymbol{f}}$ as given in (3.4). For this a posteriori error estimator we can establish the following reliability result.

**Theorem 3.3** (Reliability). *Let $(\boldsymbol{u}, p, s, c)$ and $(\boldsymbol{u}_h, p_h, s_h, c_h)$ be the solutions to (1.2) and (3.4), respectively. If $\boldsymbol{u}$, $s$ and $c$ satisfy the bounds*

$$\|\boldsymbol{u}\|_{L^\infty(0,t_{\mathrm{end}};W^{1,\infty}(\Omega))} < M, \quad \|s\|_{L^\infty(0,t_{\mathrm{end}};L^\infty(\Omega))} < M, \quad \|c\|_{L^\infty(0,t_{\mathrm{end}};L^\infty(\Omega))} < M \tag{3.6}$$

*for sufficiently small M, then there exists $C > 0$, independent of h, such that*

$$\left(\|e_{\boldsymbol{u}}\|_\star^2 + \|e_s\|_\star^2 + \|e_c\|_\star^2\right)^{1/2} \leq C\mathcal{K}, \quad \mathcal{K} := \left(\Theta^2 + \int_0^{t_{\text{end}}} \|\boldsymbol{f} - \boldsymbol{f}_h\|_{0,\Omega}^2 \,\mathrm{d}t\right)^{1/2},$$

$$\|\partial_t e_{\boldsymbol{u}} + \nabla(p - p_h)\|_{L^2(0,t_{\text{end}};\boldsymbol{H}^{-1})} + \|\partial_t e_s\|_{L^2(0,t_{\text{end}};H^{-1})} + \|\partial_t e_c\|_{L^2(0,t_{\text{end}};H^{-1})} \leq C\mathcal{K},$$

*where we define* $\|\boldsymbol{v}\|_\star^2 := \|\boldsymbol{v}\|_{L^\infty(0,t_{\text{end}};L^2(\Omega))}^2 + \int_0^{t_{\text{end}}} \|\boldsymbol{v}\|_{1,\mathcal{T}_h}^2 \,\mathrm{d}t$ *and* $\|\phi\|_\star^2 := \|\phi\|_{L^\infty(0,t_{\text{end}};L^2(\Omega))}^2 + \int_0^{t_{\text{end}}} \|\phi\|_{1,\Omega}^2 \,\mathrm{d}t.$

Finally, the result for the a posteriori error analysis for the fully discrete problem, but limited to the simpler case of backward Euler time discretization, can be formulated as follows. For each time step $k$ ($1 \leq k \leq N$), we define a global in space time indicator $\Xi_k$ by $\Xi_k := (\Xi_{k,1}^2 + \Xi_{k,2}^2 + \Xi_{k,3}^2)^{1/2}$, where

$$\Xi_{k,1}^2 := \tilde{\tau}_k\left(\|\boldsymbol{u}_h^k - I^k\boldsymbol{u}_h^{k-1}\|_{1,\mathcal{T}_{h,k}}^2 + h_e\tilde{\tau}_k^{-2}\|[\![I^k\boldsymbol{u}_h^{n-1} - \boldsymbol{u}_h^{n-1}]\!]\|_{0,e}^2 + h_e\tilde{\tau}_k^{-2}\|[\![\boldsymbol{u}_h^n - I^k\boldsymbol{u}_h^{n-1}]\!]\|_{0,e}^2\right),$$

$$\Xi_{k,2}^2 := \tilde{\tau}_k\|s_h^k - s_h^{k-1}\|_1^2, \quad \Xi_{k,3}^2 := \tilde{\tau}_k\|c_h^k - c_h^{k-1}\|_1^2,$$

where $I^k$ is generic data transfer operator which depends on the specific implementation [19]. We may now define the cumulative time and spatial error indicators

$$\Xi^2 := \sum_{k=1}^N \Xi_k^2, \quad \Upsilon^2 := \sum_{k=1}^N \tilde{\tau}_k\left(\Upsilon_k^2(\boldsymbol{u}_h^k, p_h^k, s_h^k, c_h^k) + \Upsilon_k^2(I^k\boldsymbol{u}_h^{k-1}, I_p^k p_h^{k-1}, s_h^{k-1}, c_h^{k-1})\right), \tag{3.7}$$

terms $\Upsilon_k^2$ are constructed with the a posteriori error estimator contributions defined as in the steady case (3.3), but at a given time step $k$. That is, $\Upsilon_k^2(\boldsymbol{u}_h^k, p_h^k, s_h^k, c_h^k) = \Upsilon_{K,k}^2 + \Upsilon_{e,k}^2 + \Upsilon_{J,k}^2$ with

$$\Upsilon_{K,k}^2 := h_K^2\left(\|\boldsymbol{R}_K^k\|_{0,K}^2 + \|R_{1,K}^k\|_{0,K}^2 + \|R_{2,K}^k\|_{0,K}^2\right), \quad \Upsilon_{e,k}^2 := \sum_{e\in\partial K} h_e\left(\|\boldsymbol{R}_e^k\|_{0,e}^2 + \|R_{1,e}^k\|_{0,e}^2 + \|R_{2,e}^k\|_{0,e}^2\right),$$

$$\Upsilon_{J,k}^2 := \sum_{e\in\partial K} h_e^{-1}\|[\![\boldsymbol{u}_h^k]\!]\|_{0,e}^2;$$

the residual terms are not written out here; they are similar to the stationary case but include time differences.

**Theorem 3.4** (Reliability estimate). *Let $(\boldsymbol{u}, p, s, c)$ be the solution of (1.2), and $(\boldsymbol{u}_h, p_h, s_h, c_h)$ the corresponding discrete solution. If $\boldsymbol{u}$, s and c satisfy the bounds (3.6), then the following reliability estimate holds:*

$$\begin{aligned}&\left(\int_0^{t_{\text{end}}} \left[\|\boldsymbol{e}_\tau^{\boldsymbol{u}}\|_{1,\mathcal{T}_h}^2 + \|e_\tau^c\|_{1,\Omega}^2 + \|e_\tau^s\|_{1,\Omega}^2\right] \mathrm{d}t\right)^{1/2} \\ &\quad + \sum_{k=1}^N \left(\|\partial_t \boldsymbol{e}_{\tilde{\tau}}^{\boldsymbol{u}} + \nabla(p - p_h)\|_{L^2(t_{k-1},t_k;\boldsymbol{H}^{-1}(\Omega))} + \|\partial_t e_{\tilde{\tau}}^s\|_{L^2(t_{k-1},t_k;H^{-1}(\Omega))} + \|\partial_t e_{\tilde{\tau}}^c\|_{L^2(t_{k-1},t_k;H^{-1}(\Omega))}\right) \\ &\leq C\left(\Xi^2 + \Upsilon^2 + \frac{1}{2}\|\boldsymbol{e}_{\tilde{\tau}}^{\boldsymbol{u}_c}(0)\|_{0,\Omega}^2 + \frac{1}{2}\|e_{\tilde{\tau}}^s(0)\|_{0,\Omega}^2 + \frac{1}{2}\|e_{\tilde{\tau}}^t(0)\|_{0,\Omega}^2 + \sum_{k=1}^{N-1} \|u_{h,r}^k - I^{k+1}u_{h,r}^k\|_{0,\Omega}^2 + \Theta^2\right)^{1/2}.\end{aligned}$$

## 4 | NUMERICAL TESTS

In Example 1, a known analytical solution is used to verify theoretical convergence rates of the scheme. We focus on the lowest-order method with $k = 1$ and choose $t_{\text{end}} = 1$ and $\Omega = (0,1)^2$. We take the parameter values $\nu = \exp(-c)$,

**TABLE 1** Example 1. Experimental errors and convergence rates for $\boldsymbol{u}_h$, $p_h$, $s_h$ and $c_h$ for the lowest-order method ($k = 1$).

| DoFs | $h$ | $\Delta t$ | $e_u$ | rate | $e_p$ | rate | $e_s$ | rate | $e_c$ | rate |
|---|---|---|---|---|---|---|---|---|---|---|
| 59 | 0.7071 | 0.5000 | 1.15e+01 | — | 1.36e+02 | — | 8.46e-02 | — | 1.71e-01 | — |
| 195 | 0.3536 | 0.2500 | 5.14e+00 | 1.16 | 5.73e+01 | 1.25 | 5.44e-02 | 0.64 | 1.17e-01 | 0.54 |
| 707 | 0.1768 | 0.1250 | 2.16e+00 | 1.25 | 2.09e+01 | 1.46 | 3.08e-02 | 0.82 | 6.75e-02 | 0.80 |
| 2691 | 0.0884 | 0.0625 | 9.50e-01 | 1.19 | 8.00e+00 | 1.38 | 1.63e-02 | 0.92 | 3.60e-02 | 0.90 |
| 10499 | 0.0442 | 0.0312 | 4.37e-01 | 1.12 | 3.28e+00 | 1.29 | 8.38e-03 | 0.96 | 1.86e-02 | 0.95 |
| 41475 | 0.0221 | 0.0156 | 2.08e-01 | 1.07 | 1.42e+00 | 1.21 | 4.24e-03 | 0.98 | 9.45e-03 | 0.98 |

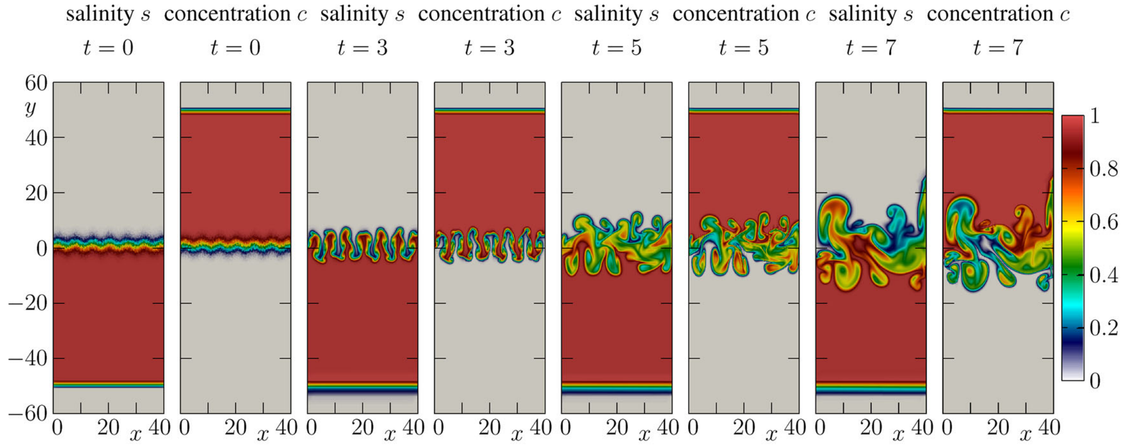


**FIGURE 1** Simulation of salinity $s$ and particle concentration $c$ at times $t = 0$ (initial datum), $t = 3$, 5, and 7.

$\rho = \rho_{\mathrm{m}}(\alpha s + \beta c)$, $\alpha = 1$, $\beta = 1$, $\rho_{\mathrm{m}} = 1.5$, $\boldsymbol{g} = (0, -1)^T$, $\mathrm{Sc} = 1$, $\tau = 0.5$, $v_p = 1$, and $a_0 = 50$. Following the approach of manufactured solutions, we prescribe boundary data and additional external forces and adequate source terms so that the closed-form solutions to (1.1) are given by the smooth functions

$$u(x,y,t) = (\cos(\pi x)\sin(\pi y)\sin(t), -\sin(\pi x)\cos(\pi y)\sin(t))^{\mathrm{T}}, \quad p(x,y,t) = \cos(x+y)\sin(x-y)\sin(t),$$

$$c(x,y,t) = (0.5 + 0.5\cos(\pi(x+y)/2))\exp(-t), \quad s(x,y,t) = (0.5 + 0.5\sin(\pi(x-y)/2))\exp(-t).$$

As $\boldsymbol{u}$ is prescribed everywhere on $\partial\Omega$, for sake of uniqueness we impose $p \in L^2_0(\Omega)$ through a real Lagrange multiplier approach. To verify the a priori error estimates, we introduce the discrete norms

$$|||\boldsymbol{u}|||_{0,\mathcal{T}_h} := \left(\Delta t(\|\boldsymbol{u}_h^1\|^2_{1,\mathcal{T}_h} + \cdots + \|\boldsymbol{u}_h^N\|^2_{1,\mathcal{T}_h})\right)^{1/2}, \quad |||\chi|||_{0,k} := \left(\Delta t(\|\chi_h^1\|^2_{k,\Omega} + \cdots + \|\chi_h^N\|^2_{k,\Omega})\right)^{1/2}.$$

The corresponding individual errors and convergence rates are $e_{\boldsymbol{u}} = |||\boldsymbol{u} - \boldsymbol{u}_h|||_{0,\mathcal{T}_h}$, $e_p = |||p - p_h|||_{0,0}$, $e_s = |||s - s_h|||_{0,1}$, $e_c = |||c - c_h|||_{0,1}$ and $\text{rate} = \log(e_{(\cdot)}/\tilde{e}_{(\cdot)})[\log(\xi/\tilde{\xi})]^{-1}$, $\xi = \{h, \Delta t\}$, where $e, \tilde{e}$ denote errors generated on two consecutive pairs of mesh size and time step $(h, \Delta t)$, and $(\tilde{h}, \tilde{\Delta t})$, respectively. For $\Delta t = \sqrt{2}h$ and the scheme (2.4), the results in Table 1 confirm that the rates of convergence are optimal, coinciding with the theoretical bounds anticipated in Theorem 2.7.

In Example 2 we illustrate the model and the proposed method by simulating salinity-driven flow motivated by the treatments in refs. [14, 26]. We consider a rectangular domain of dimensions $L_x = 40$ and $L_y = 300$ and the initial solid-particle concentration profile $s(x,y) = A_0 \exp(-y^2/\sigma^2) + A_1 \sin(x)$ with initial amplitudes $A_0$ and $A_1$ and width $\sigma$ (see Figure 1). For the velocity field, we use a non-slip boundary condition on all four walls and choose $\Delta t = 0.1$. Since simulations at low density ratios are costly because of the large Reynolds numbers of fingering convection (cf. [26]), we choose an initial density ratio $R_0 = \alpha s_{0,z}/\beta c_{0,z} \approx 4$ and simulate a tall, thin domain. Apart from the specifications above, we set $A_0 = 2.86$, $A_1 = 0.5$, $\sigma = 0.35$, $\nu = 10^{-3}\,\mathrm{kg/m^3}$, $g = 9.8\,\mathrm{m/s^2}$, $\mathrm{Sc} = 7.0$, $\tau = 25$, $v_{\mathrm{p}} = 0.04\,\mathrm{m/s}$, $\alpha = -2.0$, and $\beta = 0.5$. According to [26] a linear fingering instability occurs provided $1 < R_0 < \tau$, hence the instability shown in Figures 1 and 2 is expected. For this test an adaptive refinement is applied guided by the estimators in (3.7).

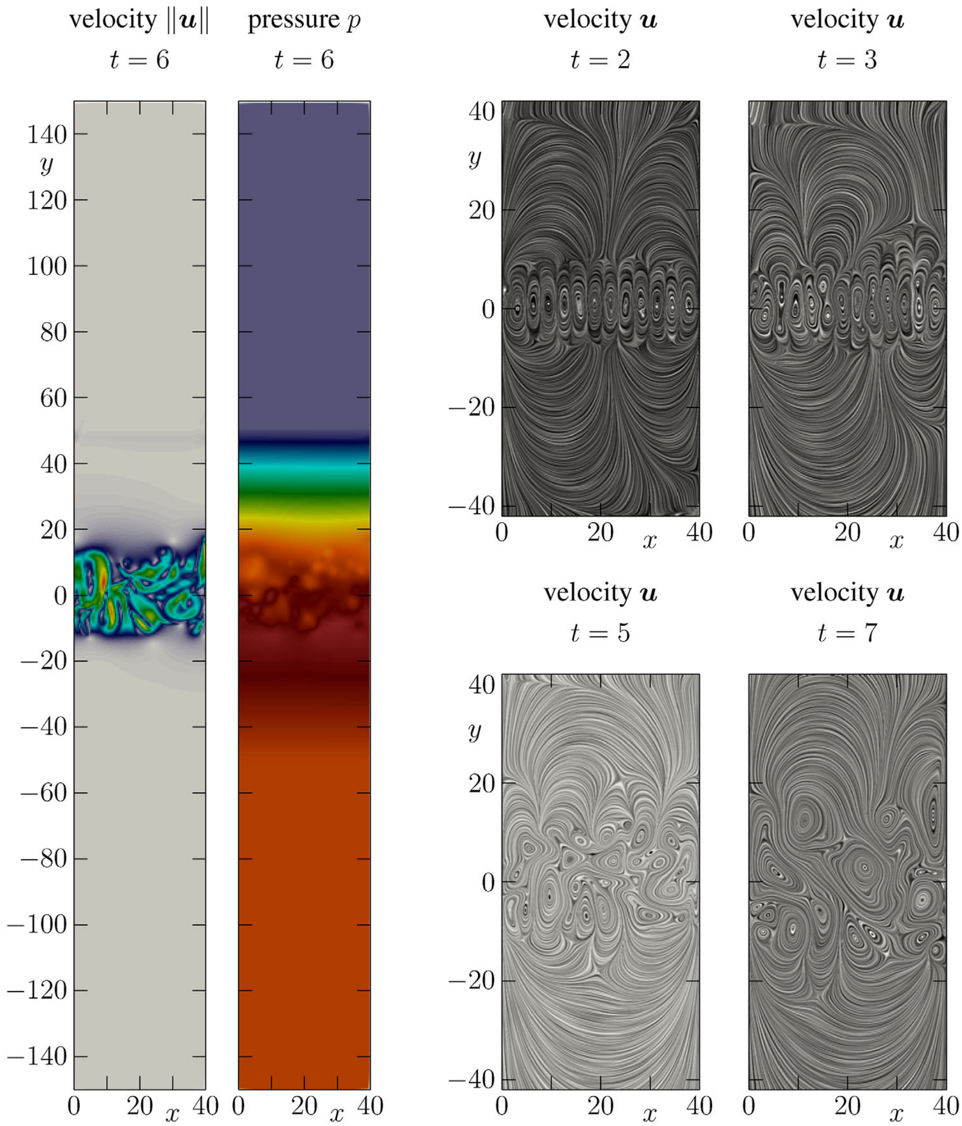


**FIGURE 2** Simulated norm of velocity $\|\boldsymbol{u}\|$ and pressure $p$ on the whole computational domain (left) and line integral convolution plots of the simulated velocity field $\boldsymbol{u}$ at $t = 2, 3, 5$, and 7 (right).

## ACKNOWLEDGMENTS

This work has been supported by ANID (Chile) through projects Fondecyt 1210610; CMM, FB210005 of BASAL funds for centers of excellence; CRHIAM, ANID/FONDAP/15130015 and ANID/FONDAP/1523A0001; and Anillo ANID/ACT210030; by the Sponsored Research & Industrial Consultancy (SRIC), IIT Roorkee, India through the faculty initiation grant MTD/FIG/100878; by SERB MATRICS grant MTR/2020/000303; by SERB Core research grant CRG/2021/002569; by the Monash Mathematics Research Fund S05802-3951284; by the Ministry of Science and Higher Education of the Russian Federation within the state support for the creation and development of World-Class Research Centers DIGITAL BIODESIGN AND PERSONALIZED HEALTHCARE No. 075-15-2022-304; and by the Australian Research Council through FUTURE FELLOWSHIP grant FT220100496 and DISCOVERY PROJECT grant DP22010316.

## ORCID

*Raimund Bürger* https://orcid.org/0000-0001-9298-8981

## REFERENCES

1. Agroum, R. (2017). A posteriori error analysis for solving the Navier-Stokes problem and convection-diffusion equation. *Numerical Methods for Partial Differential Equations*, *34*, 401–418.

2. Aldbaissy, R., Hecht, F., Mansour, G., & Sayah, T. (2018). A full discretisation of the time-dependent Boussinesq (buoyancy) model with nonlinear viscosity. *Calcolo*, *55*, 44–49.
3. Allendes, A., Naranjo, C., & Otárola, E. (2020). Stabilized finite element approximations for a generalized Boussinesq problem: A posteriori error analysis. *Computer Methods in Applied Mechanics and Engineering*, *361*, 112703.
4. Alvarez, M., Gatica, G. N., & Ruiz-Baier, R. (2016). A posteriori error analysis for a viscous flow-transport problem. *ESAIM: Mathematical Modelling and Numerical Analysis*, *50*, 1789–1816.
5. Alvarez, M., Gatica, G. N., & Ruiz-Baier, R. (2018). A posteriori error estimation for an augmented mixed-primal method applied to sedimentationconsolidation systems. *Journal of Computational Physics*, *367*, 322–346.
6. Anaya, V., Bendahmane, M., Mora, D., & Ruiz-Baier, R. (2018). On a vorticity-based formulation for reaction-diffusion-Brinkman systems. *Networks and Heterogeneous Media*, *13*, 69–94.
7. Arnold, D. N., Brezzi, F., Cockburn, B., & Marini, L. D. (2002). Unified analysis of discontinuous Galerkin methods for elliptic problems. *SIAM Journal on Numerical Analysis*, *39*, 1749.
8. Baird, G., Bürger, R., Méndez, P. E., & Ruiz-Baier, R. (2021). Second-order schemes for axisymmetric Navier–Stokes–Brinkman and transport equations modelling water filters. *Numerical Mathematics*, *147*, 431–479.
9. Bernardi, C., El Alaoui, L., & Mghazli, Z. (2014). A posteriori analysis of a space and time discretization of a nonlinear model for the flow in partially saturated porous media. *IMA Journal of Numerical Analysis*, *34*, 1002–1036.
10. Braack, M., & Richter, T. (2007). From experiments via mathematical modeling to numerical simulation and optimization. In: *Reactive flows, diffusion and transport* (W. Jäger, R. Rannacher, & J. Warnatz Eds.). Springer-Verlag.
11. Brezzi, F., Douglas, J., & Marini, L. D. (1985). Two families of mixed finite elements for second order elliptic problems. *Numerical Mathematics*, *47*, 217–235.
12. Bürger, R., Khan, A., Méndez, P. E., & Ruiz-Baier, R. (2024). Divergence-conforming methods for transient double-diffusive flows: a priori and a posteriori error analysis. *IMA Journal of Numerical Analysis*, in press.
13. Bürger, R., Méndez, P. E., & Ruiz-Baier, R. (2019). On H(div)-conforming methods for double-diffusion equations in porous media. *SIAM Journal on Numerical Analysis*, *57*, 1318–1343.
14. Burns, P., & Meiburg, E. (2015). Sediment-laden fresh water above salt water: nonlinear simulations. *Journal of Fluid Mechanics*, *762*, 156–195.
15. Cangiani, A., Georgoulis, E. H., & Sabawi, M. (2020). A posteriori error analysis for implicit explicit hp-discontinuous Galerkin timestepping methods for semilinear parabolic problems. *Journal of Scientific Computing*, *82*, 26.
16. Dallmann, H., & Arndt, D. (2016). Stabilized finite element methods for the Oberbeck–Boussinesq model. *Journal of Scientific Computing*, *69*, 244–273.
17. Danaila, I., Moglan, R., Hecht, F., & Le Masson, S. (2014). A Newton method with adaptive finite elements for solving phase-change problems with natural convection. *Journal of Computational Physics*, *274*, 826–840.
18. Dib, S., Girault, V., Hecht, F., & Sayah, T. (2019). A posteriori error estimates for Darcy's problem coupled with the heat equation. *Mathematical Modelling and Numerical Analysis*, *53*, 2121–2159.
19. Georgoulis, E. H., Lakkis, O., & Virtanen, J. M. (2011). A posteriori error control for discontinuous Galerkin methods for parabolic problems. *SIAM Journal on Numerical Analysis*, *49*, 427–458.
20. Girault, V., & Raviart, P. A. (1986). *Finite element methods for Navier–Stokes equations: Theory and algorithms*. Springer-Verlag.
21. Karakashian, O. A., & Jureidini, W. N. (1998). A nonconforming finite element method for the stationary Navier–Stokes equations. *SIAM journal on numerical analysis*, *35*, 93–120.
22. Könnö, J., & Stenberg, R. (2011). H (div)-conforming finite elements for the Brinkman problem. *Mathematical Models and Methods in Applied Sciences*, *21*, 2227–2248.
23. Larson, M. G., Söderlund, R., & Bengzon, F. (2008). Adaptive finite element approximation of coupled flow and transport problems with applications in heat transfer. *International Journal for Numerical Methods in Fluids*, *57*, 1397–1420.
24. Lenarda, P., Paggi, M., & Ruiz-Baier, R. (2017). Partitioned coupling of advection-diffusion-reaction systems and Brinkman flows. *Journal of Computational Physics*, *344*, 281–302.
25. Rakotondrandisa, A., Sadaka, G., & Danaila, I. (2020). A finite-element toolbox for the simulation of solidliquid phase-change systems with natural convection. *Computer Physics Communications*, *253*, 107188.
26. Reali, J. F., Garaud, P., Alsinan, A., & Meiburg, E. (2017). Layer formation in sedimentary fingering convection. *Journal of Fluid Mechanics*, *816*, 268–305.
27. Wilfrid, H. K. (2019). An a posteriori error analysis for a coupled continuum pipe-flow/Darcy model in Karst aquifers: anisotropic and isotropic discretizations. *Results in Applied Mathematics*, *4*, 100081.
28. Woodfield, J., Alvarez, M., B.Gomez-Vargas, R. & Ruiz-Baier, (2019). Stability and finite element approximation of phase change models for natural convection in porous media. *Journal of Computational and Applied Mathematics*, *360*, 117–137.


**How to cite this article:** Bürger, R., Khan, A., Méndez, P. E., & Ruiz-Baier, R. (2024). A divergence-conforming method for flow and double-diffusive transport. *Proceedings in Applied Mathematics and Mechanics*, e202400201. https://doi.org/10.1002/pamm.202400201